2016

Loop Heat Pipes and mini-Vapour Cycle System for Helicopter Avionics Electronic Thermal Management

Claudio Zilio
Dept. of Management and Engineering, University of Padova, Italy, claudio.zilio@unipd.it

Simone Mancin
Dept. of Management and Engineering, University of Padova, Italy, simone.mancin@unipd.it

Romain Hodot
Thales avionics, France, romain.hodot@fr.thalesgroup.com

Claude Sarno
Thales avionics, France, claude.sarno@fr.thalesgroup.com

Vincent Pomme
Airbus Helicopter, Fran, vincent.pomme@airbus.com

See next page for additional authors

Authors
Claudio Zilio, Simone Mancin, Romain Hodot, Claude Sarno, Vincent Pomme, and Bertrand Truffart

Loop Heat Pipes and mini-Vapour Cycle System for Helicopter Avionics Electronic Thermal Management

Claudio ZILIO[1]*, Simone MANCIN[1], Romain HODOT[2], Claude SARNO[2], Vincent POMME[3], Bertrand TRUFFART[3]

[1] University of Padova, Department of Management and Engineering,
Vicenza, Italy
Ph. +39-0444998746, claudio.zilio@unipd.it

[2] Thales Avionics, Navigation Packaging,
Valence Cedex, France

[3] Airbus Helicopter, ECS & Thermal Departments,
Marignane, France

* Corresponding Author

ABSTRACT

With the increase of heat flux densities generated by electronics, manufacturers are facing tremendous new challenges in which component heat flux might reach 100 W/cm². This scenario is pushing the research efforts towards the development of alternative solutions, which will be able to ensure the needed cooling demands of high-integrated electronics. Furthermore, when considering the aeronautical applications, the reliability, compactness, and lightness of the cooling systems represent essential and mandatory characteristics. With the continuous miniaturization of the components, passive and active two-phase cooling devices can now be applied to electronics systems while maintaining the fundamental compactness and lightness of the whole system. This paper presents the experimental assessment of an electronic cooling prototype especially designed for helicopter avionics thermal management in the framework of 7th FP EU project TOICA (Thermal Overall Integrated Conception of Aircraft, www.toica-fp7.eu).
The prototype consists of a set of compact Loop Heat Pipes (LHPs) especially designed for the hot spot treatment at blade level and an air cooled mini-Vapor Cycle System (mini-VCS), which is devoted to the overall heat rejection. One innovative concept of this system design lies in the presence of a thermal connector, named thermal plug, which acts as the evaporator of the mini-VCS, that cools down the LHP condenser. The experimental results are carried out at different hot spot heat loads, from 10 W to 50 W. The effect of different heat sink temperatures on the LHP thermal resistance is investigated. Furthermore, for a fixed evaporating temperature of the mini-VCS, the effects of vapor superheating at the outlet of the plug evaporator on the LHP thermal resistance is investigated. The proposed preliminary results allow to exploit the potentiality to use the proposed cooling technology in a typical airborne scenario.

1. INTRODUCTION

As the number of electrical and electronic systems increases, their physical sizes decrease, and the spacing between electrical components decreases, both the total amount of heat generated (hence to be dissipated) and the power density (the heat generated per unit volume) increase significantly. There is a general agreement in the scientific community that current air-cooling technologies are asymptotically approaching their limits imposed by available cooling area, available air flow rate, fan power, and noise (Wei *et al.*, 2007, Webb, 2007, and Kandlikar and Grande, 2004). Consequently, the thermal management architecture of aeronautical electronic packaging needs to be significantly stretched to meet these challenges (Hodot, 2015; PRIMAE, 2012).
Integrated Modular Avionics (IMA) represents real-time computer network airborne systems. This network consists of a number of computing modules capable of supporting numerous applications of different criticality levels.

One of the first steps for the development of IMA concept is probably represented by the work of the F-22 Joint Integrated Avionics Working Group (JIAWG) 30 years ago (Gaska *et al.*, 2015). Basically, the approach aims at replacing numerous separate processors and line replaceable units (LRUs) with fewer, more centralized processing units. This brings about a significant weight reduction and maintenance savings in both military and commercial airborne platforms. Since the last three decades, the IMA concept has been more and more largely applied to military and commercial aircrafts (including the most recent Airbus A380 and A350, and Boeing 787) and helicopters (Gaska *et al.,* 2015; Guilianton and Germanetti, 2011). A picture of a typical IMA design and of a blade tested in this paper are reported in Figure 1.

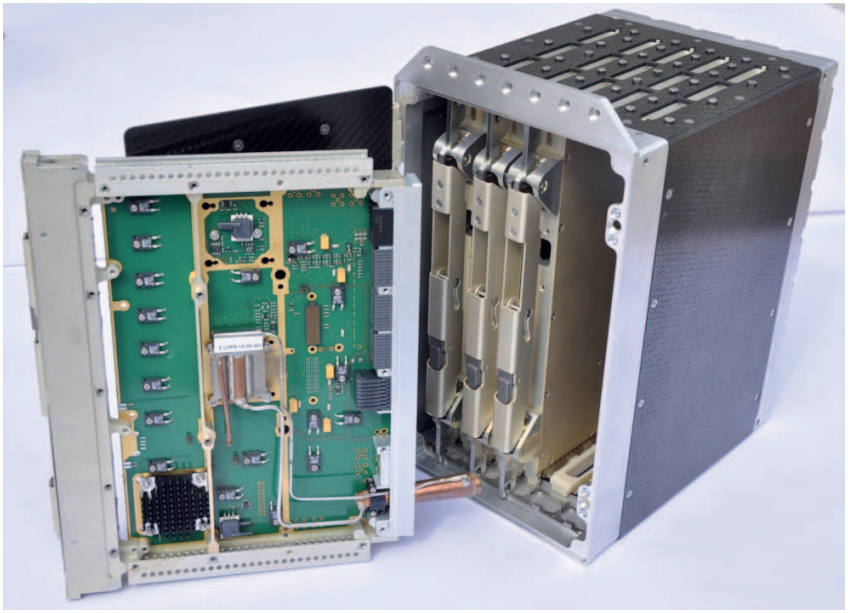

Figure 1: Picture of the tested IMA

Given the particular blade architecture and the CPUs locations on it, the thermal management of "hot spots" is very often a critical issue and dedicated thermal management strategies must be implemented to convey the heat from the hot spot to the heat sink. In the open literature several possible solutions have been proposed among these, the use of loop heat pipes (LHP) for thermal management of avionics was proposed in several applications. For instance, Maydanik *et al.* (2010) tested a LHP for cooling an electronic box installed beneath the seat of a commercial aircraft. The LHP condenser was cooled by forced liquid circulation. The authors demonstrated that it was possible to handle at the LHP evaporator up to 100 W (6.25 W cm^{-2}). They found that the hot spot temperature increases when increasing the condenser heat sink temperature. Furthermore, for a given LHP orientation, the total thermal resistance of the LHP was governed by the condenser heat transfer efficiency.
It is worth to highlight that the particular airborne applications consider ambient temperatures up to 70 °C and using the ambient air as the heat sink brings about high hot spot temperatures. On the contrary, lower hot spot temperature values ensure higher reliability for the electronics. Considering the particularly harsh environmental conditions that can occur in aeronautical constraints (ambient temperature up 70 °C), one opportunity is the use of a Vapor Cycle System (VCS) refrigerator by coupling the VCS evaporator with the LHP condenser. The possibility of using compact and lightweight VCS for avionics cooling was outlined in Mancin *et al*. (2013).
The present integration concept of a LHP installed at blade level with a mini-VCS was developed within the TOICA Project (Thermal Overall Integrated Concept Aircraft, www.toica-fp7.eu). Figure 2a represents the new delocalized modular cooling unit, where the IMA can be installed in several positions inside a helicopter and the heat from the hot spots is conveyed to a delocalized mini-VCS. Figure 2b shows, at blade level, the use of a LHP to convey the heat flow rate from an electronic component (hot spot) to the LHP condenser (female thermal plug in the picture) that is located on the back-side wall of the IMA case. Then a female-to-male thermal plug (named Plug Evaporator) adsorbs the heat , being the solid thermal bridge from the LHP and the VCS. In Figure 2b, a possible configuration with three LHPs and as many plug evaporators of the mini-VCS is depicted. Thanks to the delocalization of the condensing unit of the mini-VCS it is possible to use suitable remote heat sinks (ambient air or liquid loops, when

available) to reject the VCS condensation heat flow rate.
One innovative concept of this system design lies in the presence of a thermal connector, named thermal plug or plug evaporator, which acts as the evaporator of the mini-VCS, that cools down the LHP condenser (Hodot *et al*, 2015). This particular design presents some critical aspects. In fact, it is well known that the operation temperature of the heat source connected to the evaporator of the LHP is a function of the operating conditions of the LHP itself (including, among others, LHP condenser heat sink temperature, heat source heat flow rate, inclination, etc.). When changing one of the LHP operating conditions, normally a new working set of working temperatures are reached. Nevertheless, it can be assumed that a "true" stable LHP operation is never reached and temperatures can float continuously with the possibility of oscillatory behavior in some working conditions. This aspect has been investigated by several authors (see for example, Ku *et al*., 2001, Celata *et al.,* 2010) but no studies about the use of a VCS evaporator as heat sink for a LHP condenser have been proposed.
The VCS evaporator performance is affected by several parameters like the heat flux (or the heat source temperature), the refrigerant evaporation temperature, the refrigerant vapor superheating at the evaporator outlet, the refrigerant mass flux, etc. Furthermore, to the authors knowledge, there is no evidence in the literature about the performance of conical bayonet-type evaporators with operating conditions requested by the aeronautical constraints.
Within TOICA a thermal management system prototype was built and tested. In this paper emphasis is given to the impact of the main operating parameters of the female-to-male plug (i.e. the VCS plug evaporator) on the temperature reached by the hot spot under different operating conditions.
In order to highlight the operating peculiarities of both LHP and mini-VCS plug evaporator, the two heat transfer devices were firstly investigated separately and then they were coupled to analyze their behavior in a "real" operating condition.

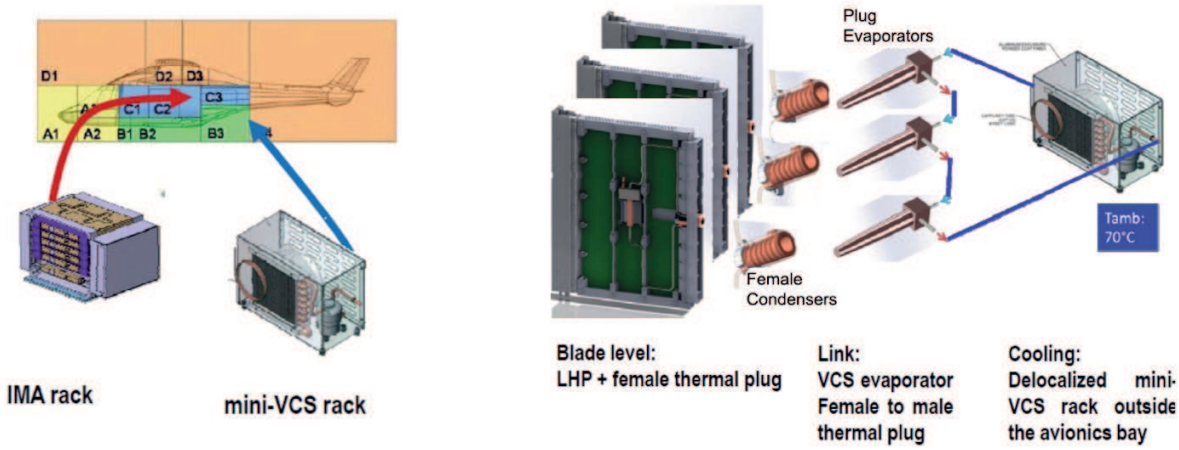

(a) **(b)**

Figure 2: Delocalized modular cooling unit concept

2. MODULAR AVIONICS COOLING DEMOSTRATOR

In the following, after a short outline of typical airborne operating conditions, the thermal performance requirements are reported together with the main characteristics of the demonstrator.

2.1 Airborne operating conditions

In the framework of the integration of new equipment item in an helicopter, the aircraft manufacturer has to demonstrate that the equipment item is operational in the whole flight domain of the helicopter, and that its integration will not have a thermal impact on other equipment items or system.
For new helicopters programs, three principal thermal requirements are need:

- The first is the OAT (Outside Air Temperature) domain in operating: the temperature justification of the helicopter should cover the following OAT domain in operation :

  - -45 °C in cold weather (if possible no damage with cold soak at -50°C),
  - +55 °C in hot weather.
- The second is the storage at low temperature : to cover H/C transport in cargo plane, the storage condition at H/C level should be -55°C.
- The third is the storage at high temperature : the most severe climatic conditions in parking conditions are OAT=55°C and solar flux = 1120 W m^{-2}.

In DO-160 (2010) term, the specification associated to this kind of equipment item in ventilated avionic bays is the following:

Table 1: DO160 specifications for helicopters.

	Ambient T	**Inlet T**	**Outlet T**	**duration**	**Equipment state**
Continuous limitation	70°C(*)	55 °C(*)	70°C	infinite	ON
Transient limitation	85°C	TBD	TBD	30 minutes	ON
Storage	-45°C / 85°C	-45°C/ 85°C	-45°C /85°C	infinite	OFF

These values are adapted to a conventional cooling design by ventilation of an equipment item. Using new cooling technics should allow to integrate this equipment in a more severe thermal environment.

2.2 Thermal performance requirements

The thermal performance requirements are linked to those of the electronic components. To ensure good component reliability and lifetime, the junction temperature must not exceed 125 °C at steady-state and temperature difference at the component surface must not exceed 3 K. A large temperature difference at the electronic component surface leads to excessive thermo-mechanical stresses. This specification is linked to the ability of the LHP saddle to spread the heat flux over its surface in contact with the component. The electronic component can bear higher temperature values during short transients. The maximum junction temperature is linked to the performance of the whole system, LHP, contact resistance between the plug, and mini-VCS.

For the LHP, these requirements are expressed in terms of minimum heat flux at which the device starts up, maximum temperature difference between the heat source and the condenser, and maximum temperature difference at the component surface. As heat fluxes up to 20 W can be dissipated by classical cooling technologies without exceeding the maximum allowed junction temperature, the LHP start-up must occur at a minimum heat flux of 20 W. The LHP thermal performance is specified for two operating modes: in nominal conditions, when the applied heat flux is 50 W (nominal power), and in degraded mode, corresponding to a short transient state or when the LHP is operated above its nominal power.

2.3 Demonstrator characteristics

The IMA demonstrator depicted in figure 1 was considered with the LHP installed inside the blade. A plane electrical heater (3 x 3 cm^2) was placed at the center of the blade and the LHP attached on it. As it can be seen, the evaporator is made of copper with cylindrical shape. The cylinder is soldered onto an aluminum saddle for suitable coupling with the plane heater. The compensation chamber is made of stainless steel and the lines connecting the evaporator with the condenser are made of stainless steel (vapor line internal diameter 2 mm, liquid line internal diameter 1.5 mm) . The copper condenser is obtained by a spirally grooved channel inserted inside a conical female sheath. The condenser channel length is 0.488 m, with grooves of 2.5 × 2 mm^2. The exchange area between the male and female plug is 15.9 cm^2. Given the relatively small dimensions listed above, the present LHP can be considered a miniature device, according to Singh *et al.* (2007).

In normal operation, the LHP is designed for up to 50 W heat flow rate, with the possibility of short transient loads up to 80 W.

The compressor of the mini-VCS is a variable speed unit (ASPEN 19-24-100X). Three evaporators operate in parallel, and a micro-metering valve is used as throttling device. The evaporators are bayonet-type heat exchangers designed as male plugs for the LHP condenser. Pictures of plug evaporators and LHP condenser are reported in Figure 3.

Figure 3: Pictures of the tested LHP condenser (left-hand side) and mini-VCS plug evaporator (right-hand side).

3. EXPERIMENTAL RESULTS

As previously described, the LHP and the thermal plugs were preliminarily studied to assess their performance independently; then the components were coupled and the whole system was experimentally tested at a fixed evaporating temperature and compressor speed. This section reports these preliminary experimental results separately to clearly present the general assessment of the prototypes.

3.1 LHP experimental analysis.

One plug heat exchanger was fed with water from a thermostatic bath that controlled the set water inlet temperature within ±0.05 K. As reported in Figure 4, 11 calibrated T-type thermocouples (probe diameter 0.4 mm) were attached in different locations of the LHP (uncertainty (k= 2) within ±0.1 K) and one thermocouple was inserted between the heater and the LHP evaporator to measure the heart temperature, T_{HEART}. This temperature can be thus considered as representative of the actual hot spot temperature.
The blade was then inserted in the IMA box with the LHP having condenser-up/evaporator-down orientation.

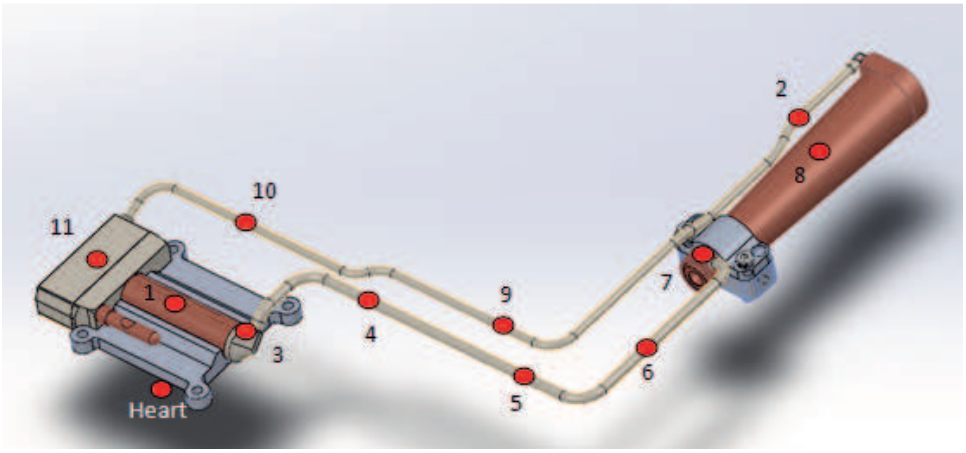

Figure 4: Position of the thermocouples along the LHP. Heart is the sensor between the heater and the evaporator. 1 is over the evaporator, 8 is over the condenser. 3 is evaporator outlet, 2 is condenser outlet.

The LHP evaporator to heater thermal coupling was accomplished by adding high thermal conductivity silicon grease (declared thermal conductivity 3 W $m^{-1}K^{-1}$) and ensuring a sufficient mechanical bonding by means of 4 screws.
The plug was inserted in the LHP condenser and the same silicon grease was used. To meet the avionic maintenance and replacement requirements, no further mechanical coupling devices were used. An additional 0.4 mm T-type thermocouple was placed between the LHP condenser and plug evaporator in order to record the interface material

temperature. Tests were run with the IMA at ambient temperature at around 23 °C. The heat load was increased from 10 W to 50 W by means of a stabilized DC supply (stability ±0.05 W) to the flat electrical heater installed in the middle of the blade (hot spot). The heat load was indirectly measured by means of a calibrated reference resistance (shunt) and by the measurement of the effective electrical potential difference (EDP) of the resistance (heater). From Ohm's law, since the resistance is known, it is possible to calculate the current from the measured potential difference. So, the effective power supplied to the hot spot was evaluated with two accurate EDP measurements. The estimated accuracy of the electrical power supplied (heat load) is within ±0.15% of the measured value.

In Figure 5, the recorded profiles of the heart temperature (T_{HEART}) at heat load up to 50 W are plotted together with the temperature at the interface ($T_{interface}$) between the plug and the LHP condenser and with the water inlet temperature ($T_{w,i}$). The water inlet temperature was changed from 5 °C to 30 °C. The cooling water mass flow rate was set to allow a water temperature gain across the plug always lower than 3 K.

At a glance, the heart temperature (T_{HEART}) decreases as the heat sink temperature decreases. Furthermore, it can be seen that heat sink temperatures up to 30 °C allow a safe operation of the electronics (considering that 130 °C is the maximum allowable temperature for transient operations). It is also evident that the difference between the heart temperature (T_{HEART}) and the interface temperature ($T_{interface}$) is much lower than the difference between the interface temperature ($T_{interface}$) and the water inlet temperature ($T_{w,i}$). Finally, no relevant instabilities in the LHP temperatures were retrieved at the present working conditions.

It is possible to define three "conventional" thermal resistances as follows:

$$R_{TOT} = (T_{HEART} - T_{w,i})/\text{HEAT LOAD} \quad (1)$$

$$R_{LHP} = (T_{HEART} - T_{interface})/\text{HEAT LOAD} \quad (2)$$

$$R_{interface} = (T_{interface} - T_{w,i})/\text{HEAT LOAD} \quad (3)$$

R_{TOT} is representative of the whole thermal resistance, while R_{LHP} can be considered as representative of the LHP thermal resistance, whereas $R_{interface}$ can be used to exploit the thermal resistance due to the plug heat transfer performance.

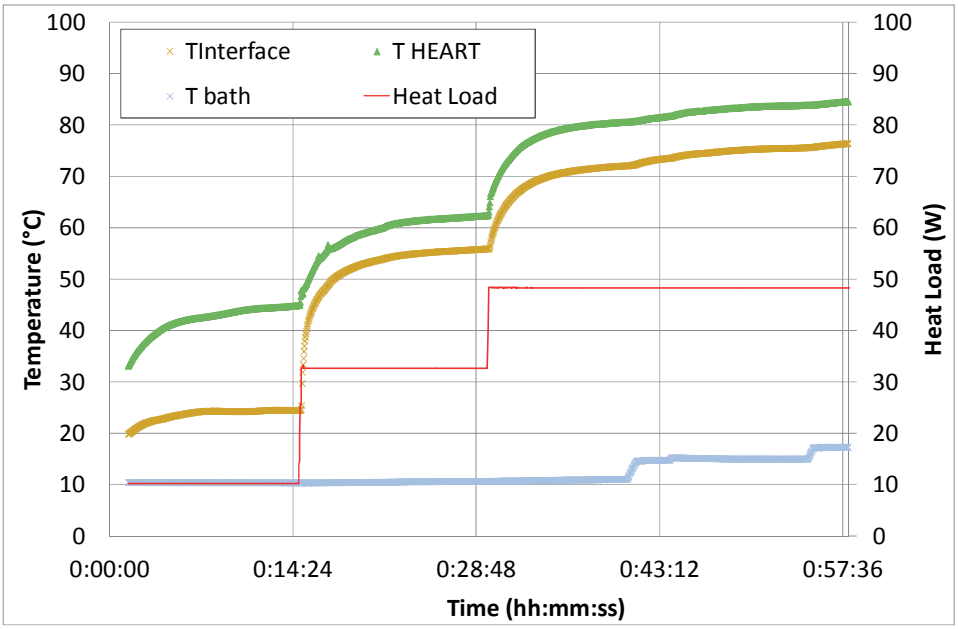

Figure 5: Temperature profiles as a function of the hot spot heat load and of the water inlet temperature.

R_{TOT} was found to be 1.26 K W^{-1} when the inlet water temperature was 30 °C and it was found to increase up to 1.52 K W^{-1} when the water temperature decreased down to 5 °C. $R_{interface}$ was found to be equal to 1.10 K W^{-1} when the inlet water temperature was 30 °C at it was found to increase up to 1.33 K W^{-1} when the water temperature

decreased down to 5 °C. The measured R_{LHP} was 0.16 K W^{-1} with $T_{w,i}$ =30°C and 0.19 k W^{-1} $T_{w,i}$ =5°C indicating a poor sensitivity to the water inlet temperature.
Accordingly, the thermal resistance due to the plug heat transfer is the most critical one when liquid cooling of the plug is used, as also stated by (Maydanik *et al*, 2010).

3.2 Mini-VCS experimental analysis at imposed temperature on the plug evaporator surface

As mentioned before, given the particular design of the LHP condenser and according to the airborne installation/replacement/maintenance requirements, the plug configuration used for this demonstrator is quite unusual and there is no evidence in the open literature about the performance of this type of conical bayonet evaporators. Furthermore, basing on the observed behavior of the LHP (Figure 5), the plug is expected to work with temperatures on the external surface up to 90 °C. To preliminary assess the performance of the plug, when operating as evaporator of the mini-VCS, three plugs were arranged in parallel and tested at fixed external surface temperature.
In order to measure all the main operating parameters of the VCS, a dedicated test rig, similar to the one proposed by Righetti *et al.* (2015) was used. The schematic of the test rig is reported in Figure 6. To match the helicopter installation requirements, a ¼" ID flexible hose 1.5 m long line (1/4" ID) was installed between the micro-metering throttling valve and the manifold, while 3 hoses, each 1 m long, were installed after the manifold to feed the bayonet type evaporators. A 2.5 m long (overall length) gas line from the plugs to the compressor was also used to close the loop.

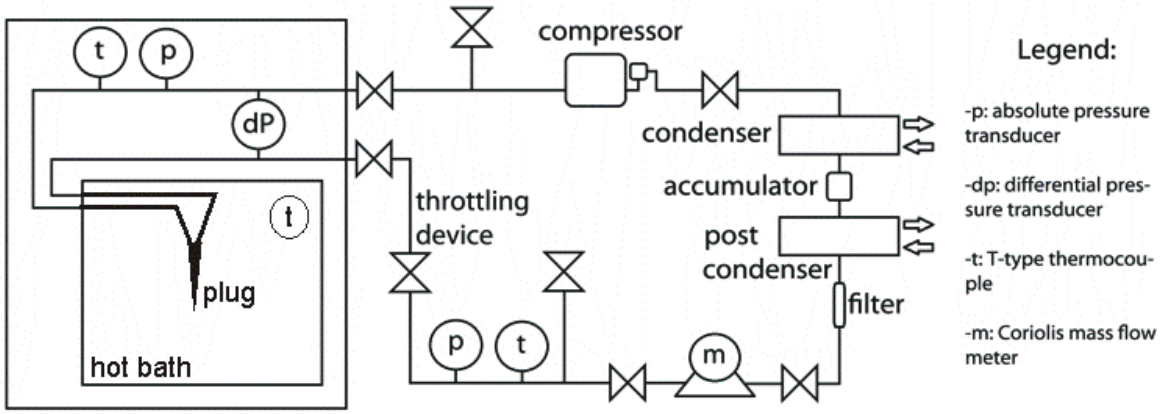

Figure 6: mini-VCS test rig.

As previously described, the compressor is a 1.9 cm^3 rotary model made by Aspen, driven by a DC brushless motor with variable speed control. The considered refrigerant is R134a.
The condenser is a water cooled tube-in-tube heat exchanger fed by a thermostatic bath; so it is possible to control the condensing temperature by controlling water-side inlet temperature and flow rate. A liquid accumulator is placed after the condenser to ensure the necessary amount of refrigerant during high load tests. Once out of the condenser, the subcooled liquid finds a filter then it passes through the throttling device.
The refrigerant mass flow rate was measured by a Coriolis effect mass flow meter (uncertainty (k = 2) within ±0.1 % of the reading). Two strain gauge absolute pressure transducers were positioned at the outlet of the evaporator (uncertainty (k = 2) within ± 0.075% f.s.; f.s= 10 bar), at the inlet of the throttling device (uncertainty (k= 2) within ± 0.075% f.s.; f.s= 20 bar) respectively. In addiction two T-type thermocouples (uncertainty (k = 2) within ±0.1 K) were placed inside adiabatic mixing chambers, one just before the throttling valve and one at the evaporator outlet. Thanks to the measured temperatures and pressures it is possible to evaluate specific enthalpy and refrigerant quality at the evaporator inlet and the specific enthalpy at the evaporator outlet.
To simulate the typical temperatures at the plug surface measured during the LHP experimental characterization (see Figure 5), the three plugs were immerged in a thermostatic bath. The bath temperature was set at 66 ± 0.1 °C.
It is well known that the heat flow rate exchanged by an evaporator at fixed heat sink temperature is a function of the evaporation temperature, of the vapor superheating, of the inlet vapor quality, and of the refrigerant mass flow rate (or mass flux, being fixed the evaporator geometry and circuitry). Figure 7a reports the measured heat flow rate when the refrigerant mass flow rate was changed as in Figure 7b, while keeping the vapor superheating fixed at 3 K.

For all the reported data-points the condensation temperature was set at 44 °C with 6 °C to 7 °C condensate subcooling. Figure 7a also reports the vapor quality at the evaporator inlet.
From the analysis of the diagrams, at fixed condensation pressure and liquid temperature, the inlet vapor quality decreases as a consequence of an increase of evaporation temperature. This, in turn, has a positive effect on the plug evaporator performance. In fact, as it can be seen, when decreasing the inlet vapor quality, it is possible to achieve higher heat flow rate by also increasing the evaporation temperature, still being fixed the heat sink temperature. This aspect is evidently favorable for the whole performance of the mini-VCS (the higher the evaporation temperature, the lower the compressor work, for a given condensation temperature).

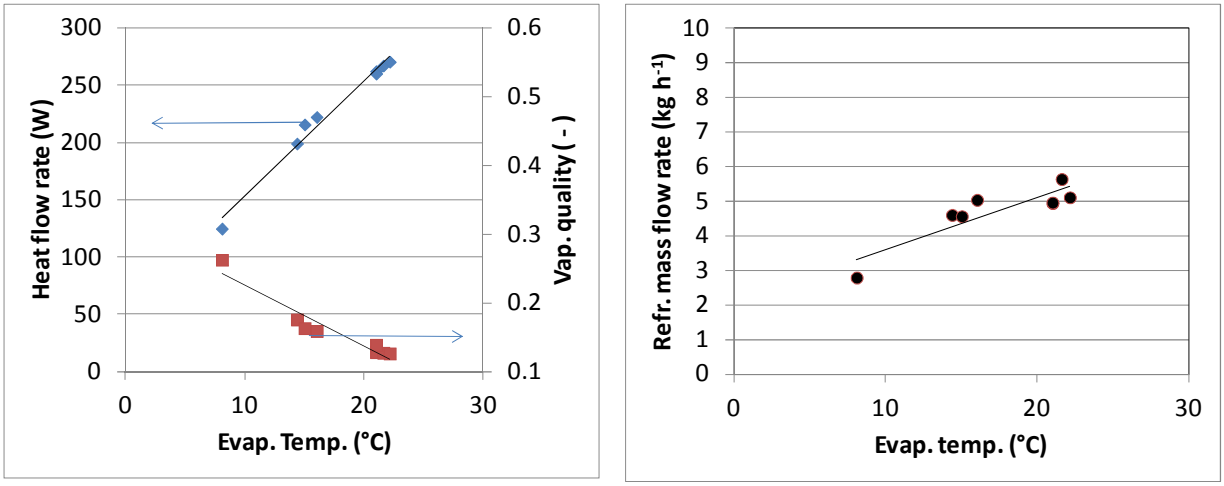

(a) (b)

Figure 7: Plug evaporator performance as a function of evaporation temperature and inlet vapor quality (a) and the corresponding measured mass flow rate (b) at fixed vapor superheating (3 K).

In order to assess the heat transfer capabilities of the plug evaporator, Figure 8 reports the evaporation temperature and vapor superheating at the evaporator outlet as a function of the refrigerant mass flow rate. The figure refers to a constant inlet vapor quality of 0.12 and a fixed heat flow rate (270 W, i. e the maximum value reported in Figure 7a). It is worth noticing that this heat flux is more than 2.5 times higher the maximum peak value expected for the LHP condenser. For the sake of safety during LHP operation, such a high value was used cautiously for the present tests to measure the maximum heat flow rate that can be rejected by the plug evaporator for a given heat source temperature (in this case 66 °C).
In Figure 8 it can be seen that it is possible to increase the evaporation temperature up to 21.5 °C by increasing the refrigerant mass flow rate. As it can be expected, this causes a decrease of the vapor superheating. At 21.5 °C evaporation temperature, a further increase of the refrigerant mass flow rate has the only consequence of decreasing the vapor superheating to a limiting value of about 2 K (a further decrease of the vapor superheating can be considered a limit condition, from the point of view of possible liquid return to the compressor in real system operation).

3.3 Mini-VCS – LHP experimental analysis

After the preliminary independent assessment of the LHP and of the plug evaporators, the complete modular cooling unit (LHP + mini-VCS) was coupled and then investigated.
During this test, the condensation saturation temperature was fixed at 38.5 °C, with 8 K liquid subcooling. The evaporator saturation temperature changed during the tests from 5 °C to 6 °C. Accordingly, the refrigerant vapor quality at the evaporator inlet changed from 0.18 and 0.19. The vapor superheat at the compressor suction changed from 2 K to 10 K. The compressor running speed was kept constant. According to the above listed operating conditions, the total refrigerant mass flow rate ranged from 3.4 kg h^{-1} to 3.6 kg h^{-1}. Three plug evaporators were fed in parallel by means of the micro-metering hand settled throttling valve. The imposed heat load at the LHP was fixed at 40 W.

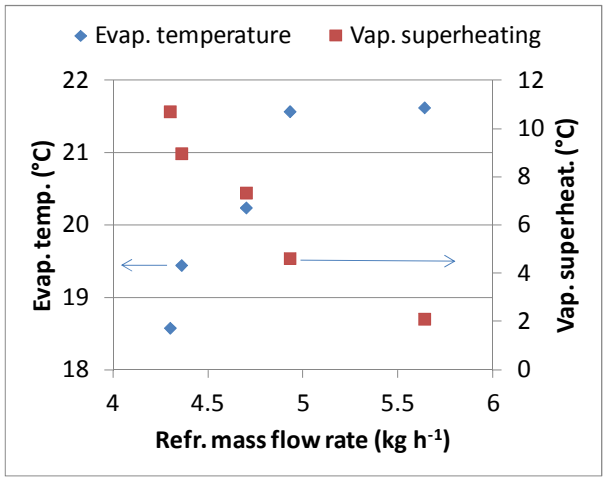

Figure 8: Effects of refrigerant mass flow rate, evaporation temperature, vapor superheating at fixed heat flow rate (270 W) and inlet vapor quality (0.12).

In this configuration, the definitions of the thermal resistances given in equations 1 and 3, are modified as follows, to account for the evaporation temperature ($T_{ev,sat}$) calculated according to the saturation pressure measured at the evaporator outlet:

$$R_{TOT} = (T_{HEART} - T_{ev,sat})/\text{HEAT LOAD} \quad (4)$$

$$R_{interface} = (T_{interface} - T_{ev,sat})/\text{HEAT LOAD} \quad (5)$$

At an evaporation temperature of 5 °C with a vapor superheating at the evaporator outlet equal to 2 K, $R_{interface}$ was found to be very low (0.06 K W^{-1}) thanks to the beneficial effect of R134a boiling heat transfer. This results in a reduction of the total thermal resistance R_{TOT}. In fact, it was measured to be 1.13 K W^{-1} instead of 1.52 K W^{-1} as measured with the water cooled plug at 5°C water inlet temperature (-23%). The advantage is evident on the hot spot temperature; T_{HEART} was 53.2 °C instead of 65.8 °C previously reached.
Furthermore, it is important to outline the effect of R134a vapor superheating at the plug outlet. At the same evaporation temperature, but with 5 K vapor superheating, $R_{interface}$ increased to 0.70 K W^{-1} since part of the evaporator operated in single phase conditions with rather lower heat transfer coefficients on the refrigerant side. As a consequence, R_{TOT} increased to 1.50 K W^{-1} with T_{HEART}=66.7 °C, showing a performance similar to the liquid cooled plug with $T_{w,i}$ = 5 °C.
When increasing the vapor superheating up to 10 K, R_{TOT} increased to 1.67 K W^{-1} with T_{HEART}=71.3 °C as a consequence of the higher value of $R_{interface}$ (1.22 K W^{-1}) caused by the relevant vapor superheating. However, it is important to observe that the operating temperatures of the hot spot can be considered safe in any tested working condition.

4. CONCLUSIONS

A new delocalized modular cooling unit for the thermal management of hot spots inside an IMA box for aeronautical applications was proposed. Experiments were carried out to exploit the effect of the main working parameters on the thermal resistance of a LHP that conveys the heat generated by a local hot spot inside one of the IMA blades towards a conical bayonet-type plug evaporator that is integrated in a delocalized mini-VCS operating with R134a.
The tests showed that the proposed architecture is worth of future research investigation for proper integration in avionics cooling strategies. The mains advantages for the air framer are the following: no filtration required at equipment level as the heat is evacuated out of the box through conduction, only one area where the ventilation has to be secured, the avionics bay could be insulated which is an advantage in parking conditions with high solar heat fluxes. This new cooling technology offer promising performances, above state of the art with up to 55°C benefit at 40 W as compared to classical cooling system.

NOMENCLATURE

OAT	Outside Air Temperature	(°C)	R	Thermal Resistance (K/W)
T	Temperature	(°C)		

Subscript

ev,sat	evaporation temperature
HEART	Heart
interface	Interface
LHP	Loop Heat pipe
TOT	Total
w,i	Water inlet

REFERENCES

Celata, G.P., Cumo, M., Furrer, M. (2010). Experimental tests of a stainless steel loop heat pipe with flat evaporator, Exp. Th. Fluid Science, 34, 866-878.

DO-160 (2010). Environmental Conditions and test Procedures for Airborne Equipment, Radio Technical Commission of Aeronautics (RTCA), Washington DC.

Hodot, R. (2015). Modeling and test of loop heat pipes for civil and military avionic applications. PhD Thesis, Institut National des Sciences Appliquées de Lyon.

Hodot, R., Sarno, C, Zilio, C, Mancin, S, Pomme, V, Truffart, B. (2015). Electronic cooling for avionics using loop heat pipes and mini-Vapour Cycle Systems. IMAPS, La Rochelle, France.

Gaska, T., Watkin, C., Chen, Y. (2015). Integrated Modular Avionics—Past, Present, and Future, IEEE A&E Systems Magazine (Sept.), 12–23

Guilianton, E., Germanetti, S. (2011). System architecture for new avionics on eurocopter fleet based on IMA supporting civil and military missions, 37th European Rotorcraft Forum 2011, Vergiate and Gallarate; Italy.

Kandlikar, S., Grande W. (2004). Evaluation of single phase flow in microchannels for high flux chip cooling Thermodynamic performance enhancement and fabrication technology, Proc.of 2nd Int. Conf. on Microchannels and Minichannels (67-76).

Ku, J., Ottenstein, L., Kobel, M., Rogers, P., Kaya, T. (2001). Temperature oscillations in loop heat pipe operation, AIP Conference Proceedings 552 (1), 255–262

Mancin, S., Zilio, C., Righetti, G., Rossetto, L. (2013). Mini Vapor Cycle System for high density electronic cooling applications. Int. J Refrigeration, 36, 1191- 1202.

PRIMAE (2012). The Packaging of futuRe Integrated ModulAr Electronics research project. Contract n. 265413. From: http://cordis.europa.eu/result/rcn/57808_en.html

Righetti, G., Zilio, C., Longo, G.A. (2015). Comparative performance analysis of the low GWP refrigerants HFO1234yf, HFO1234ze(E) and HC600a inside a roll-bond evaporator, Int. J Refrigeration, 54, 1-9.

Singh, R., Akbarzadeh, A., Dixon, C., Mochizuki, M., Riehl, R.R. (2007), Miniature loop heat pipe with flat evaporator for cooling computer CPUs, IEEE Transactions on Components and Packaging Technologies 30 (1).

Maydanik, Y. F., Vershinin, S., Pastukhov, V.G., Chernysheva, M., Sarno, C., Tantolin, C. (2010). Passive cooling system for an aircraft electronic box, Heat Pipe Science and Technology, 1(3), 251-260.

Webb, R., (2007). Next generation devices for electronic cooling with heat rejection to air. J. of Heat Transfer, 127, 2-9.

Wei, X., Joshi, Y., Patterson M.K. (2007), Experimental and numerical study of stacked microchannel heat sink for liquid cooling of microelectronic devices. J. of Heat Transfer, 129, 1432-1444.

ACKNOWLEDGEMENT

This research project was partially funded by the European Commission within the framework of the research Project, TOICA (Thermal Overall Integrated Conception of Aircraft), contract n. ACP3-GA-2013-604981.